

Dielectric and optical properties of a poly(ethylene terephthalate) membrane in the temperature interval 150–400 K

Slavica B. Maletic,¹ Dragana D. Cerovic,^{1,2} Filip S. Marinkovic,¹ Jablan R. Dojcilovic¹

¹Faculty of Physics, University of Belgrade, Studentski trg 12, 11000, Belgrade, Serbia

²College of Textile Design, Technology, and Management, Starine Novaka 24, 11000, Belgrade, Serbia

Correspondence to: S. Maletic (E-mail: sslavica@ff.bg.ac.rs)

ABSTRACT: In this study, the dielectric and optical properties of poly(ethylene terephthalate) (PET) membranes were examined. The dielectric measurements were carried out in the temperature interval 150–400 K and in the frequency range 20 Hz–60 kHz. We analyzed in detail the temperature dependences of the dielectric permittivity and dielectric loss ($\tan \delta$) at various test frequencies. The relaxation $\tan \delta$ peak, which appeared in the temperature range 150–300 K, was identified as the secondary β relaxation. The increase in $\tan \delta$ at temperatures higher than 300 K could be explained as approaching the α relaxation. Optical measurements were performed in the UV–visible region from 200 to 400 nm at various temperatures between 150 and 400 K. The values of the direct and indirect band gaps were calculated at various temperatures. These values were lower for higher temperatures. An absorption peak was observed at a wavelength around of 285 nm at temperatures lower than 300 K. Such insight into the dielectric and optical responses of PET track membranes in a wide temperature range is particularly important when this material is used as a matrix for the semiconductor structure in the development of optoelectronic or microfluid devices. © 2015 Wiley Periodicals, Inc. *J. Appl. Polym. Sci.* **2015**, *132*, 42834.

KEYWORDS: dielectric properties; membranes; optical properties; polyesters; spectroscopy

Received 16 March 2015; accepted 12 August 2015

DOI: 10.1002/app.42834

INTRODUCTION

Poly(ethylene terephthalate) (PET) is a polyester that has (1) a high melting point because of the presence of an aromatic ring and (2) a very good mechanical strength. It is semicrystalline in nature, resistant to heat and moisture, and virtually unattached by many chemicals.^{1,2} The high transmission in the visible range makes PET a substrate that is suitable and useful for a number of applications, including optoelectronic and other thin film applications.^{3–5}

Polymeric etch track membranes are thin polymer films with discrete pores that are formed through a combination of heavy ion bombardment and chemical etching.^{3,6} Track membranes can serve as templates for making various microstructures and nanostructures.^{5,7,8} The use of ion track polymer membranes as template matrices with known nanosizes and microsized topology allows the formation of hybrid structures with highly reproducible parameters. Therefore, controlled variations in the matrix properties of PET (chemical composition, pore size, shape, and density), size, and material of nanocrystals embedded into the track pores provide broad opportunities for the development of new nanocrystal-based composite materials.⁷

The inner surface of the track pores can be modified by different chemical and electrochemical methods; this is important for the production of a variety of microfluidic devices, including pH-sensitive microfluidic diodes and biosensors.

Because of the significant technical application of PET track membranes, it is very important to determine their dielectric and optical properties as a function of temperature. Dielectric spectroscopy is a nondestructive technique that provides relevant information about the molecular dynamics in polymer systems. It is one of the most suitable methods for investigating relaxation processes.

Optical absorption measurements are widely used to specify the electronic properties of materials through the determination of parameters that describe the electronic transitions, such as optical band gap energy (E_g) and valence band tails.⁹ The absorption of light energy by polymeric materials in UV–visible regions involves the transition of electron in n , π , and σ orbitals (where n , π , and σ are designations for molecular orbitals) from the ground state to high-energy states, which are described by molecular orbitals.¹⁰ In the literature,⁷ nanocrystal CdSe/ZnS localization in the loosened layer on the PET track micrometer-sized pore wall surfaces along with empty track pores were presented.

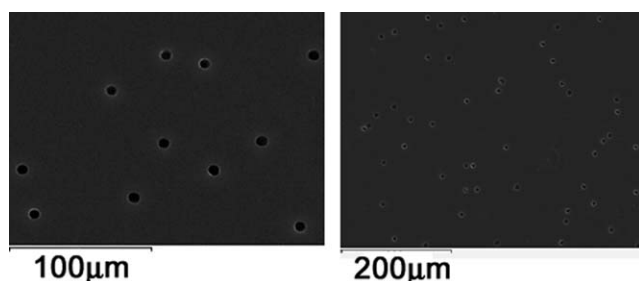


Figure 1. Scanning electron microscopy micrographs of the PET track membranes.

This material, as a matrix for the different semiconductor structures that can link molecule hosts in the surface layer of pores, is a good candidate for application in the development of optoelectronic devices or microfluidic sensors. For the development of such devices or similar ones, PET track membranes require optical characterization in a wide temperature range.

The formation of the PET membrane from PET foils leads to the cracking of long molecular chains and structure disruption of the PET film, especially near the pores and on the surface of the walls of the pores.⁷ At the polymer chain break points, carboxyl groups are formed on the inner surface and in the loosened layer on the track pore wall surface. As a result, possible changes may be expected in the dielectric and optic responses of the materials.

The results of different dielectric property measurements of PET materials of various structures can be found in the literature.^{11–14} Some of the optical characteristics of PET materials have been reported in literature.^{15,16} However, the relation between the optical characteristics of the PET track membrane and the temperature has been studied very little.

The main scope of this study was the analysis of the temperature dependences of the dielectric and optical properties of the PET track membrane. This was carried out with dielectric and UV–visible spectroscopy. The dielectric parameters of the PET membrane were studied in a broad temperature interval (150–400 K) and in the frequency range from 20 Hz to 60 kHz. The values of the direct and indirect band gaps were estimated at various temperatures from 150 to 400 K.

EXPERIMENTAL

PET track membranes were produced from the polymer foils [average molecular weight (N) = $(1.3 \pm 0.16) \times 10^5$] with the ion track-etching technique (FLNR Dubna, Russia). First, the polymer foils were irradiated with swift ions; this was followed by acid etching. PET foils were irradiated with Ar ions (energy = 1 MeV/nucleon), which passed through the foil, creating latent tracks with strongly damaged polymer chains. After irradiation, the membranes were etched in a 0.2M solution of NaOH at a temperature of 80°C. The obtained membranes were 40 μm thick with pores 7 μm in size. The scanning electron microscopy (JEOL 840 A microscope) micrograph of the PET membrane is presented in Figure 1. The pore direction relative to the foil surface was 90°. The pore density was about $2 \times 10^4 \text{ cm}^{-2}$. The crystalline properties of the sample were analyzed by

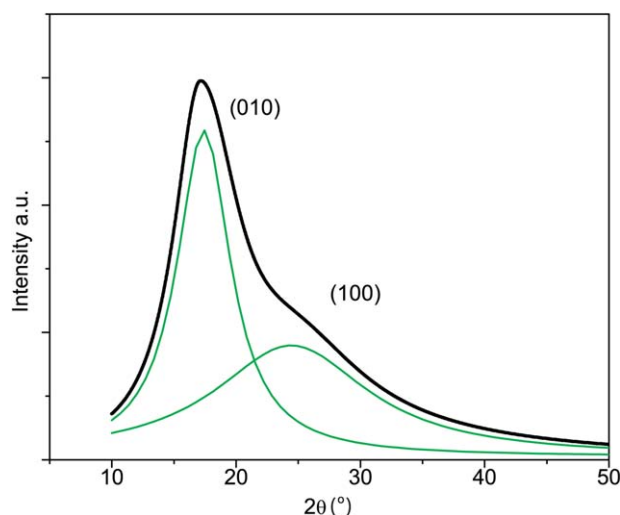


Figure 2. XRD pattern of the PET track membrane. [Color figure can be viewed in the online issue, which is available at wileyonlinelibrary.com.]

X-ray diffraction (XRD) with a Rigaku Ultima IV diffractometer in Bragg–Brentano geometry with Ni-filtered Cu $K\alpha$ radiation ($\lambda = 1.54178 \text{ \AA}$). Diffraction data were recorded over the scattering angle (2θ) from 10 to 50° with a step of 0.01° and an acquisition rate of 2°/min. A typical XRD pattern of randomized PET consisted of three peaks at 17.3° (010), 22.5° (110), and 25.7° (100).¹⁷ The XRD pattern of the investigated PET track membrane showed that the main diffraction peak at $2\theta = 17.4^\circ$ was prominent, whereas a broad peak at $2\theta = 25.3^\circ$ had a low intensity (Figure 2). These corresponded to the reflections from planes (010) and (100), respectively.

Dielectric spectroscopy measurements were carried out with a Precision LRC instrument (Hameg 8118) over a frequency range from 20 Hz to 60 kHz and a broad temperature interval from 150 to 400 K with a Lake Shore 340 temperature controller. The data acquisition was performed in heating mode with a heating rate of 2 K/min, and the applied voltage was 1 V. A sample was placed in a closed capacitor cell with cell electrodes 13 mm in diameter *in vacuo* with a pressure of 10^{-4} Pa . The samples were cut to completely cover the surfaces of the electrodes. The details of the equipment were given elsewhere.^{18–21} The conductance (G) and susceptance (B) were measured in the parallel mode capacitance (C_p) measurement model of the instrument. The instrument (Hameg 8118) was calibrated against Keithley 5155 standards (10^8 – $10^{13} \Omega$, voltage coefficient: $-0.03\%/V$).

To eliminate the parasitic capacities, two sets of G and B measurements were carried out, one set (G_m and B_m) with a sample between electrodes and another without a sample (G_b and B_b) but with a space between electrodes equal to the thickness of the sample, for the same test frequencies and at the same temperatures. The dielectric permittivity (ϵ_r) and dielectric loss ($\tan \delta$) were calculated from the experimental data with the following relations:

$$G = G_m - G_b$$

$$B = B_m - (B_b - 2\pi\epsilon_0 S/d)$$

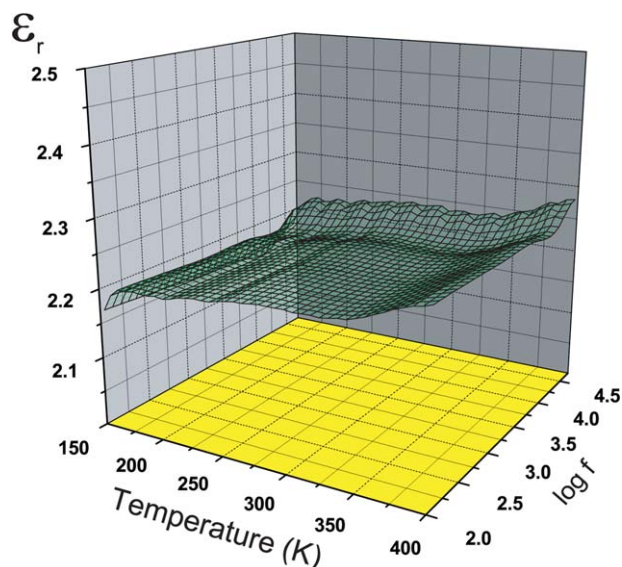


Figure 3. ϵ_r as function of the temperature and logarithm of frequency. [Color figure can be viewed in the online issue, which is available at wileyonlinelibrary.com.]

$$\begin{aligned}\tan \delta &= G/B \\ C &= B/2\pi f \\ \epsilon_r &= Cd/\epsilon_0 S\end{aligned}$$

where f is the frequency, C is the capacity, d is the spacing of the electrodes and is equal to the thickness of the sample, S is the area of the electrode, and ϵ_0 is the vacuum permittivity (8.85×10^{-12} F/m).

The transmission spectra of the PET membrane were recorded with a Shimadzu 3600 UV–visible spectrophotometer in the wavelength range from 200 to 400 nm at various temperatures

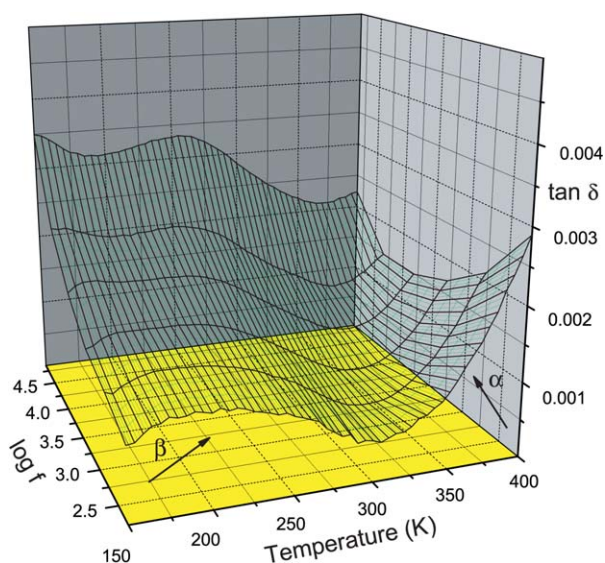


Figure 4. $\tan \delta$ as function of the temperature and logarithm of frequency. [Color figure can be viewed in the online issue, which is available at wileyonlinelibrary.com.]

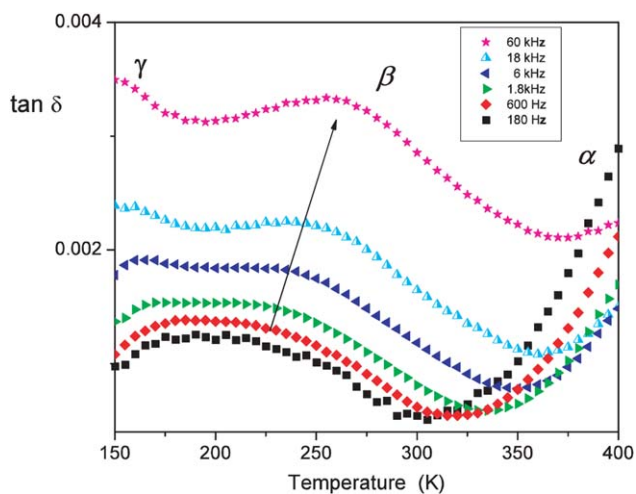


Figure 5. $\tan \delta$ of the PET membrane as a function of the temperature at various frequencies. [Color figure can be viewed in the online issue, which is available at wileyonlinelibrary.com.]

from 150 to 400 K with an Oxford Optinstant DN cryostat. We recorded the spectra starting at lower temperatures and advancing to higher temperatures. The temperature of the sample was controlled with a MercuryTC cryogenic temperature controller.

RESULTS AND DISCUSSION

Dielectric Properties

The results of the dielectric measurements of the PET track membrane are presented in Figures 3 and 4.

Figures 3 and 4 present the dependences of ϵ_r and $\tan \delta$ of the PET membrane over the frequency range from 20 Hz to 60 kHz and in the temperature range 150–400 K, respectively. Significant changes in the trend of the temperature dependences of ϵ_r were observed at temperatures of about 160 and 390 K at each tested frequency. An apparent $\tan \delta$ peak appeared in a broad temperature interval of about 150–300 K at each frequency, as shown in Figure 4.

The $\tan \delta$ peak shifted to a higher temperature with increasing frequency. In Figure 4, it is also shown that the values of $\tan \delta$ for higher temperatures (above 300 K) increased as the temperature grew at each test frequency. The start of the increase in $\tan \delta$ shifted to a higher temperature for a higher frequency.

The $\tan \delta$ relaxation peak, which appeared at about 200 K, could be identified as the secondary β relaxation. The increasing values of ϵ_r and $\tan \delta$ at temperatures higher than 350 K corresponded to the softening of the polymer and approached the glass-transition temperature. This response of the material to the applied electric field was characteristic of α relaxation.^{12,13,22}

According to the literature data,¹² the α relaxation associated with the glass-transition temperature was reported in the range of 340–410 K. This relaxation, associated with the long-range segmental motions in amorphous region, was very sensitive to the presence of a crystalline fraction.

It was characteristic of the broad peak of β relaxation that the temperature that corresponded to the peak of $\tan \delta$ was higher

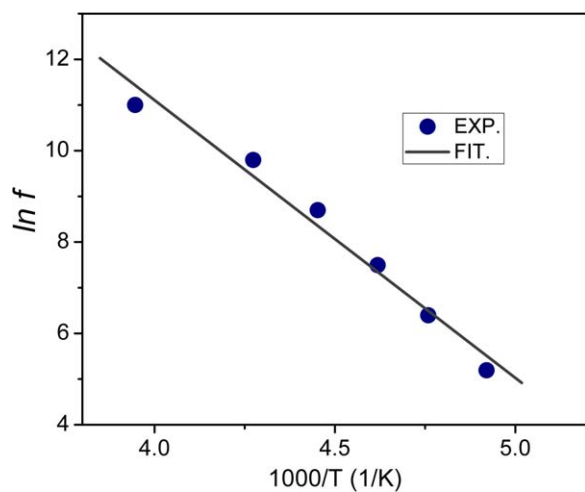


Figure 6. $\ln f$ versus $1000/T$ for β relaxation. EXP = experimental data; FIT = linear fitting. [Color figure can be viewed in the online issue, which is available at wileyonlinelibrary.com.]

for higher frequencies (Figure 5). The molecular motions in a temperature region below the glass-transition level were limited to the rotation of the side groups or parts of the side groups. The processes below the glass-transition temperature in the semicrystalline and amorphous polymeric materials were designated as β relaxation and γ relaxation. The local main chain motion formed β relaxation, and the side group motion in the repeating unit generated γ relaxation. According to the literature,¹³ the origin of β relaxation in PET was attributed to the motion of the phenyl rings and carbonyl group below the glass-transition temperature.

A detailed analysis in Figure 5 reveals a clearly visible additional $\tan \delta$ peak at a temperature of about 160 K at higher frequencies. This peak was hardly noticeable at lower frequencies and became more pronounced and more noticeable at frequencies higher than 60 kHz. Most likely, it was γ relaxation. Seemingly, the peaks of β and γ relaxation overlapped to form a broad peak at lower frequencies: 180 and 600 Hz. On the other hand, according to the authors,¹³ the relaxation that occurred at a temperature of about 160 K was accompanied by a secondary β_2 relaxation.

These results could be linked to the results of the measurements carried out on the temperature dependences of the PET material dielectric properties, which have been represented in various articles.^{13,20,23} The changes observed in the dielectric characteristics should also have been related to structural variations. Properties such as the crystallinity, orientation, and structure could have been responsible for the differences in the temperature of the relaxations.

The temperature dependence of the observed β relaxation could be described by the Arrhenius relation:

$$f = f_0 \exp(-E_a/kT) \quad (1)$$

where f is the frequency (Hz), f_0 is the pre-exponential factor, T is the absolute temperature (K), E_a is the activation energy (eV), and k is the Boltzmann constant (8.67×10^{-5} eV/K).

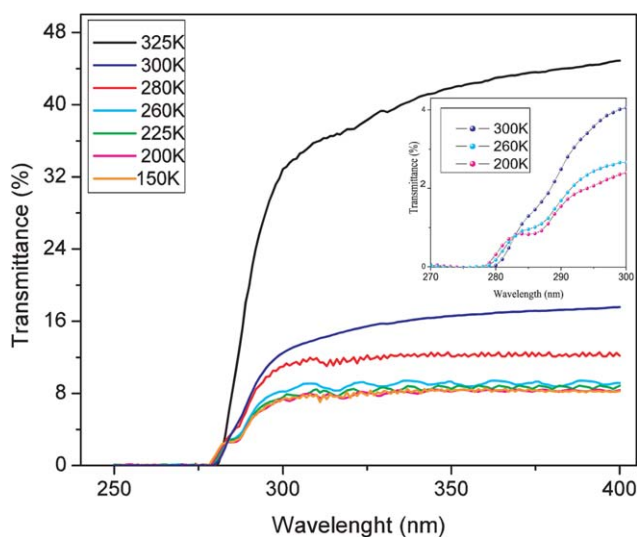


Figure 7. Transmittance of the PET membrane at various temperatures. The inset shows the absorption band around 285 nm at 200, 260, and 300 K. [Color figure can be viewed in the online issue, which is available at wileyonlinelibrary.com.]

In general, E_a acts effectively as the energy barrier of the material, which the material has to overcome to undergo the structural reorganization of the β relaxation. To determine more accurately the temperature that corresponded to the broad peak of β relaxation at lower frequencies, two Gaussians were used in the fitting of $\tan \delta(T)$ curve to resolve the overlapping of the peaks of the β and γ relaxations. Figure 6 shows the natural logarithmic dependence of the test frequencies (0.18, 0.6, 1.8, 6, 18, and 60 kHz) versus the inverse temperature ($1000/T$) of the $\tan \delta$ peak.

The best fitting line through the resulting data points yielded a slope from which the observable E_a was calculated. The obtained value of E_a was approximately 0.52 ± 0.04 eV. This value was lower than the corresponding values of PET foils from the literature,^{12,24} which were 0.71 and 0.83 eV, respectively. On the other hand, the obtained value was similar to values obtained for the porous fibrous polyethylene terephthalate structure presented in ref. 20. The lower value of E_a for the sample of the PET membrane, compared to the sample PET foil, was determined by the greater flexibility and a certain disturbance of the close packing of the macromolecules in the PET membrane. This was related to broken molecular chains or partially damaged chains. Also, the pores had a layer with partially damaged polymer chains on their walls. The loosened wall layers that formed around the pores had a lower density than the bulk polymer.⁷

Optical Properties

The transmittance spectra of the PET track membrane at different temperatures are shown in Figure 7. The absorption edge shifted slightly to a higher wavelength, that is, a lower energy, with increasing temperature. Also, an absorption band was observed in the wavelength interval of 285–290 nm. This peak gradually decreased and disappeared at temperatures higher

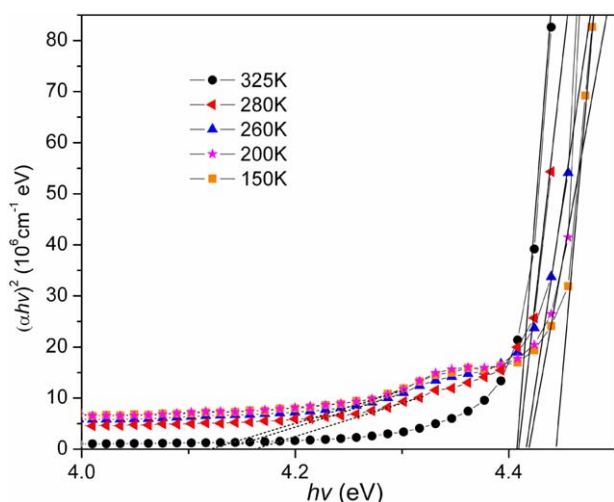


Figure 8. Dependence of $(\alpha hv)^2$ on $h\nu$ for the PET membrane at various temperatures. [Color figure can be viewed in the online issue, which is available at wileyonlinelibrary.com.]

than 300 K. Generally, the transparency of the PET sample increased with increasing temperature. A particularly noticeable increase was observed for temperatures higher than 300 K.

According to the band theory of solids, the absorption coefficient $[\alpha(\nu)]$ at different photon energies was calculated from the Urbach rule²⁵ as follows:

$$\alpha(\nu) = \left(\frac{1}{d}\right) \ln\left(\frac{100}{I_t}\right) \quad (2)$$

where I_t is the transmitted light intensity.

The relation between the optical band gap, $\alpha(\nu)$ and incident photon energy is

$$\alpha h\nu = B(h\nu - E_g)^m \quad (3)$$

where $h\nu$ is the energy of the incident photons, B is a constant, E_g is the value of the optical energy gap between the highest occupied molecular orbital (valence band) and lowest unoccupied molecular orbital (conduction bands), and m is the number that characterizes the electronic transition, both direct and indirect, during the absorption process in the k space. m values of $1/2$, $3/2$, 2 , and 3 stand for direct allowed, direct forbidden, indirect allowed, and indirect forbidden transitions, respectively.²⁶ Tauc²⁶ and Mott and Davis²⁷ independently developed the equation for optical band transition of amorphous materials establishing that the equation has the same form as eq. (3) with $m = 2$. According to the literature,¹⁰ the PET polymer follows the rules of both direct and indirect transitions.

The variations of $(\alpha hv)^2$ with photon energy for the PET membrane at different temperatures are shown in Figure 8. The intercept of the linear portion of the plot on the $h\nu$ axis gives the value of direct E_g of the membrane. The determined values are presented in Table I.

The plots of $(\alpha hv)^{1/2}$ as a function of $h\nu$ for the PET membrane are shown in Figure 9. The corresponding values are presented in Table I.

Table I. Band Gap Energy Values in the PET Membrane

Temperature (K)	Band gap energy (eV)			
	Direct		Indirect	
	E_g	E_g'	E_g	E_g'
150	4.44	4.12	4.39	3.63
200	4.42	4.12	4.39	3.63
260	4.42	4.13	4.38	3.65
280	4.41	4.16	4.35	3.74
325	4.41	-	4.34	-

We noticed that the values of the optical direct and indirect band gap slightly decreased with increasing temperature. Although small, these temperature-induced changes were not negligible, especially when PET was used as a matrix for different materials. It is important to know the matrix optical properties to correctly analyze the optical measurements performed on the embedded material plus the matrix system.

We observed, from Figures 8 and 9, that along with the energy gap between the filled valence and empty conduction band, E_g , there was a gap that was located below the investigated gap in the energy scale (E_g'). The use of the graphical method based on eq. (3) on part of the linear dependences around 4.3 eV rendered the estimate for the values of these energy gaps at different temperatures. The obtained values are presented in Table I. It was noticeable that the values increased as the temperature went up. The absorption corresponding to the additional gap disappeared at temperatures higher than room temperature, at approximately 300 K.

Generally, from the viewpoint of molecular orbitals, the electronic transitions that were involved in the UV and visible regions were of the following types: $\sigma \rightarrow \sigma^*$, $n \rightarrow \sigma^*$, $n \rightarrow \pi^*$, and $\pi \rightarrow \pi^*$. The electron transitions $n \rightarrow \pi^*$ and $\pi \rightarrow \pi^*$ were possible in the wavelength interval 200–700 nm for the PET

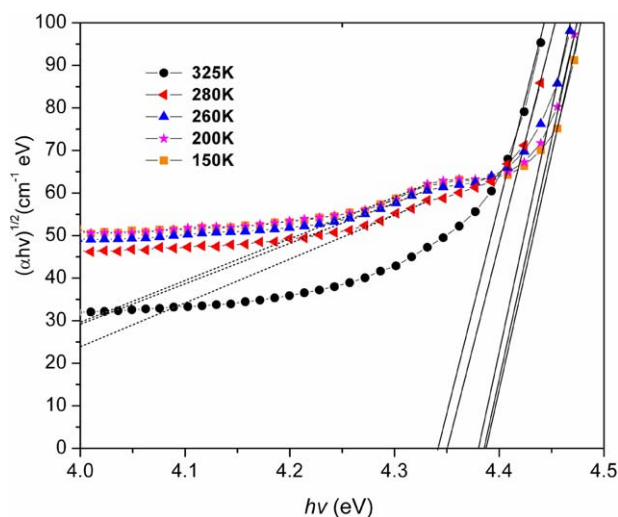


Figure 9. Dependence of $(\alpha hv)^{1/2}$ on $h\nu$ for the PET membrane at various temperatures. [Color figure can be viewed in the online issue, which is available at wileyonlinelibrary.com.]

material.²⁸ The units of the molecules that were responsible for the absorption were the most common: C=C (π to π^*) and C=O (n to π^*). A very strong absorption that occurred in the region of 270 nm was associated with the $\pi \rightarrow \pi^*$ transition.²⁹ The weak absorption band observed in the wavelength interval 285–290 nm probably corresponded to the excitation $n \rightarrow \pi^*$. With increasing temperature, all n electrons were excited, and above 300 K, this transition did not occur anymore.

CONCLUSIONS

In this study, the dielectric properties of PET track membranes were analyzed in the frequency range 20 Hz to 60 kHz and in a wide temperature interval ranging from 150 to 400 K. We established that the three relaxation processes (α , β , and γ) occurred in the polymer. The energy of activation of β relaxation was determined to be 0.52 eV. The value was lower than the corresponding value of the PET foils. The probable reason for this was that the molecular chains were discontinued or damaged, and they required less energy for overcoming potential barriers and chain reorientation. The analysis of optical properties in the wide temperature interval provided information about the change in the energy band gap of the PET membranes. The values of the direct and indirect band gaps were examined, and we established that the values of the direct gap slightly decreased with increasing temperatures in the measured temperature interval. The absorption peak of 285 nm disappeared at temperatures higher than 300 K.

The recognition and understanding of the changes that occur with a change in the temperature in the dielectric and optical properties of the PET membrane in a wide range of temperatures is particularly important because of the membrane's multiple technological applications as a substrate or matrix.

ACKNOWLEDGMENTS

This project was supported by the Science Fund of the Republic of Serbia's Ministry of Education and Science (contract grant number 171029).

REFERENCES

1. Tseng, K. S.; Lo, Y. L. *Appl. Surf. Sci.* **2013**, *285*, 157.
2. Kumar, V.; Sonkawade, R. G.; Chakarvarti, S. K.; Singh, P.; Dhaliwal, A. S. *Radiat. Phys. Chem.* **2012**, *81*, 652.
3. Liu, Q.; Yang, X.; Chen, X.; Ma, M.; Yang, K.; Liu, D.; Zhu, Z. *Polym. Int.* **2009**, *58*, 1078.
4. Choi, M. C.; Kim, Y.; Ha, C. S. *Prog. Polym. Sci.* **2008**, *33*, 581.
5. Ryu, G. S.; Jeong, S. H.; Park, B. C.; Park, B.; Song, C. K. *Org. Electron.* **2014**, *15*, 1672.
6. Spohr, R. *Radiat. Meas.* **2008**, *43*, S560.
7. Orlova, A. O.; Gromova, Y. A.; Savelyeva, A. V.; Maslov, V. G.; Artemyev, M. V.; Prudnikau, A.; Fedorov, A. V.; Baranovet, A. V. *Nanotechnology* **2011**, *22*, 455201.
8. Awasthi, K.; Kulshrestha, V.; Avasthi, D. K.; Vijay, Y. K. *Radiat. Meas.* **2010**, *45*, 850.
9. Bassani, F.; Pastori-Parravicini, G. *Electronic States and Optical Transitions in Solids*; Pergamon: Oxford, **1975**.
10. Dyer, J. R. *Applications of Absorption Spectroscopy of Organic Compounds*; Prentice-Hall: Englewood Cliffs, NJ, **1965**.
11. Sellares, J.; Diego, J. A.; Belana, J. *J. Phys. D: Appl. Phys.* **2010**, *43*, 365402.
12. Cristea, M.; Ionita, D.; Simionescu, B. C. *Eur. Polym. J.* **2010**, *46*, 2005.
13. Maxwell, A. S.; Monnerie, L.; Ward, I. M. *Polymer* **1998**, *39*, 6851.
14. Neagu, E. R.; Neagu, R. M. *J. Appl. Phys.* **2006**, *100*, 074107.
15. Guillén, C.; Herrero, J. *Mater. Chem. Phys.* **2008**, *112*, 641.
16. Ramola, R. C.; Negi, A.; Semwal, A.; Chandra, S.; Rana, J. M. S.; Sonkawade, R. G.; Kanjilal, D. *J. Appl. Polym. Sci.* **2011**, *121*, 3014.
17. Göschel, U.; Deutscher, K.; Abetz, V. *Polymer* **1996**, *37*, 1.
18. Kulagin, N.; Dojcilovic, J.; Popovic, D. *Cryogenics* **2001**, *41*, 745.
19. Maletic, S.; Maletic, D.; Petronijevic, I.; Dojcilovic, J.; Popovic, D. M. *Chin. Phys. B* **2014**, *23*, 026102.
20. Cerovic, D. D.; Dojcilovic, J. R.; Maletic, S. B. *Eur. Polym. J.* **2012**, *48*, 850.
21. Dudić, D.; Luyt, A. S.; Marinković, F.; Petronijević, I.; Dojcilović, J.; Kostoski, D. *Radiat. Phys. Chem.* **2015**, *107*, 89.
22. Bower, D. I. *An Introduction to Polymer Physics*; Cambridge University Press: Cambridge, United Kingdom, **2002**.
23. Cerović, D.; Dojcilović, J.; Petronijević, I.; Popović, D. *Con-temp. Mater.* **2014**, *1*, 42.
24. Menegotto, J.; Demont, P.; Bernes, A.; Lacabanne, C. *J. Polym. Sci. Part B: Polym. Phys.* **1999**, *37*, 3494.
25. Urbach, F. *Phys. Rev. B.* **1953**, *92*, 1324.
26. Tauc, J. *Amorphous and Liquid Semiconductors*; Plenum: New York, **1974**.
27. Mott, N. F.; Davis, E. A. *Electronic Processes in Non-Crystalline Materials*; Oxford University Press: London, **2012**.
28. Silverstein, R. M.; Clayton, B. G.; Morrill, T. C. *Spectrometric Identification of Organic Compounds*; Wiley: New York, **1981**.
29. Pavia, D. L.; Lampman, G. M.; Kriz, G. S.; Vyvyan, J. R. *Introduction to Spectroscopy*, 4th ed.; Brooks/Cole: Belmont, CA, **2009**.